



Title	Host-guest chemistry between cyclodextrin and a hydrogen evolution catalyst cobaloxime
Author(s)	Kato, Masaru; Kon, Keita; Hirayama, Jun; Yagi, Ichizo
Citation	New journal of chemistry, 43(25), 10087-10092 <a href="https://doi.org/10.1039/c9nj00081j">https://doi.org/10.1039/c9nj00081j</a>
Issue Date	2019-07-07
Doc URL	<a href="http://hdl.handle.net/2115/78820">http://hdl.handle.net/2115/78820</a>
Type	article (author version)
File Information	NJC_Co-CD_manuscript_MK13.pdf



[Instructions for use](#)

## Host–guest chemistry between cyclodextrin and hydrogen evolution catalyst of cobaloxime

 Masaru Kato,<sup>a,b\*</sup> Keita Kon,<sup>b</sup> Jun Hirayama<sup>b</sup> and Ichizo Yagi<sup>a,b\*</sup>

 Received 00th January 20xx,  
Accepted 00th January 20xx

DOI: 10.1039/x0xx00000x

www.rsc.org/

We report host–guest chemistry between cyclodextrins and a bisdimethylglyoximate cobalt complex, cobaloxime. The cobaloxime forms 1:1 host–guest assembly with  $\beta$ - or  $\gamma$ -cyclodextrin but not with  $\alpha$ -cyclodextrin. The assembly of the cobaloxime with  $\gamma$ -cyclodextrin enhances the photocatalytic hydrogen evolution activity of a homogeneous system that contains an organic dye of eosin Y in a neutral aqueous solution under visible-light irradiation.

### Introduction

Hydrogen is an attractive substitute for fossil fuels. This promising future fuel can be efficiently converted to electricity using polymer electrolyte fuel cells, which will be used for vehicles or household electricity generators.<sup>1,2</sup> A promising approach to sustainable hydrogen production is visible light-driven water splitting. Visible light-driven water splitting systems require highly efficient hydrogen evolution catalysts, which are ideally prepared from earth-abundant elements.

Many synthetic hydrogen evolution catalysts have been reported, for example, semiconductor- or molecular-based catalysts.<sup>2–7</sup> For molecular-based catalysts, hydrogen evolution with high efficiency is still a great challenge. In contrast, natural metalloenzymes such as hydrogenases show efficient inter-conversion of  $\text{H}_2/\text{H}^+$  at their active site containing earth-abundant metal complexes such as iron or nickel.<sup>8–10</sup> These enzymatic active sites are placed in cavities surrounded by peptide residues and interactions between the active site and the cavity contribute to maximizing the enzymatic activity and/or stabilizing the molecular structure of the catalytic active sites. These enzymatic active sites inspire us to mimic not only the active site structure<sup>9,11,12</sup> but also the protein environment surrounding the active site using host–guest chemistry.<sup>13–16</sup>

Herein we report host–guest chemistry of cyclodextrins as host molecules (CDs, Fig. 1) with a cobalt(III) complex of two dimethylglyoximate (Hdmg) ligands as a guest molecule (**CoPyS**, Fig. 1) and visible light-driven hydrogen evolution catalyzed by the host–guest supramolecules in water. Cobalt complexes with diglyoximate ligands, termed cobaloximes,<sup>17–23</sup> have been

studied for basic researches on hydrogen evolution<sup>4,24–31</sup> and organic synthesis<sup>32–38</sup> since they are easily synthesized, tolerant to oxygen<sup>39–41</sup> and catalytically active for photochemical or electrochemical hydrogen evolution with low overpotentials. On the other hand, CDs are cyclic oligosaccharides of 6–8 glucose units (denoted  $\alpha$ -,  $\beta$ - and  $\gamma$ -CD, respectively) and have a hydrophobic cavity and hydrophilic hydroxyl rims, providing ability to form host–guest supramolecules in water.<sup>42–45</sup> Host–guest chemistry on CDs and molecular-based catalysts will allow us to mimic active site environments in metalloenzymes and/or to gain insights into relationships between the catalytic activity of guest molecules and host–guest interactions.<sup>46–49</sup>

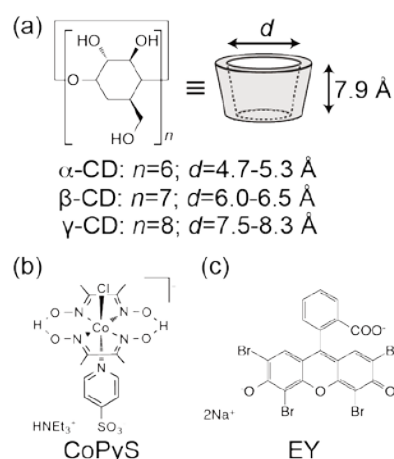


Fig. 1 Molecular structures of (a) cyclodextrins (CDs) with cavity diameters,  $d$ , (b)  $\text{HNEt}_3[\text{Co}^{\text{III}}\text{Cl}(\text{Hdmg})_2(4\text{-pySO}_3)]$  (**CoPyS**) and (c) eosin Y (**EY**). The cavity diameters are taken from Ref. <sup>50</sup>.

<sup>a</sup> Section of Environmental Materials Science, Faculty of Environmental Earth Science, Hokkaido University, N10W5, Kita-ku, Sapporo 060-0810, Japan. E-mail: masaru.kato@ees.hokudai.ac.jp

<sup>b</sup> Division of Environmental Materials Science, Graduate School of Environmental Science, Hokkaido University, N10W5, Kita-ku, Sapporo 060-0810, Japan

† Electronic Supplementary Information (ESI) available: the crystallographic data (CCDC 1447123), <sup>1</sup>H NMR spectra, time-courses of visible light-driven hydrogen evolution and cyclic voltammograms. See DOI: 10.1039/x0xx00000x

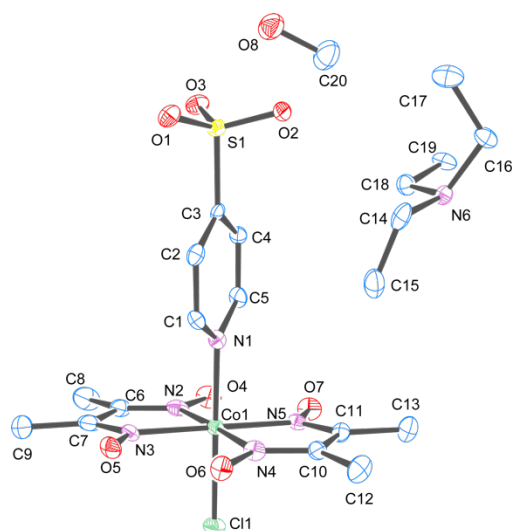


Fig. 2 ORTEP drawing of the molecular structure of  $\text{HNEt}_3[\text{Co}^{\text{III}}\text{Cl}(\text{Hdmg})_2(4\text{-pySO}_3)]\cdot\text{CH}_3\text{OH}$  showing 50% probability thermal ellipsoids and the atom-numbering scheme.

## Results and discussion

**CoPyS** was synthesized in one step from the reaction of  $[\text{Co}^{\text{III}}\text{Cl}_2(\text{Hdmg})(\text{H}_2\text{dmg})]^{51}$  with 4-pyridine sulfonic acid (4-py $\text{SO}_3\text{H}$ )<sup>52</sup> in methanol containing  $\text{NEt}_3$  at  $40^\circ\text{C}$  for 2 h (yield: 42%). The presence of the anionic sulfonate group generally increases the solubility of transition metal complexes in water and promotes inclusion of the complexes into CDs in water.<sup>46–49,53</sup> Actually, the anionic sulfonate group of  $\text{pySO}_3^-$  makes **CoPyS** soluble in water, as we expected. **CoPyS** was characterized by elemental analysis,  $^1\text{H}$  NMR, ESI-MS and single crystal X-ray analysis (See ESI<sup>†</sup>).

The single crystal X-ray analysis of **CoPyS** provides the structural information on **CoPyS**. The cobalt center has a distorted octahedral coordination geometry with two dimethylglyoximate ligands in an equatorial plane and with the ligands of 4-py- $\text{SO}_3^-$  and  $\text{Cl}^-$  in the axial position (Fig. 2). The two dimethylglyoximate ligands have intramolecular hydrogen bonding [O4...O7, 2.480(5) Å; O6...O5, 2.489(5) Å]. The sulfonate group has intermolecular hydrogen bonding with the counter cation of  $\text{HNEt}_3^+$  [N6...O3, 2.795(5) Å] and a crystal solvent of methanol [O3...O8, 2.824(5) Å].

The inclusion behavior of **CoPyS** into cyclodextrins was studied by using  $^1\text{H}$  NMR. Proton NMR spectra of **CoPyS** in  $\text{D}_2\text{O}$  showed two distinct peaks at 7.66 and 8.20 ppm in the aromatic region. These two peaks were assigned to the ortho-protons of  $\text{pySO}_3^-$  and the meta-protons, respectively. These peaks were shifted upon adding  $\beta$ -CD or  $\gamma$ -CD into the solution (Fig. S1, ESI<sup>†</sup>), indicating that these CDs formed inclusion complexes with **CoPyS**. In contrast, the addition of  $\alpha$ -CD showed no obvious change in chemical shift, implying that  $\alpha$ -CD forms no inclusion complex with **CoPyS**. These results come from size matching between **CoPyS** and CDs: the cavity of  $\alpha$ -CD (the cavity diameter  $d = 4.7\text{--}5.3$  Å) is too small to form an inclusion complex with **CoPyS** (the size of the pyridine ring: approximately 4.0 Å),

whereas the cavities of  $\beta$ -CD ( $d = 6.0\text{--}6.5$  Å) or  $\gamma$ -CD ( $d = 7.5\text{--}8.3$  Å) are large enough.<sup>50</sup>

To understand the stoichiometry of the inclusion complexes,  $^1\text{H}$  NMR spectra and ESI-MS of **CoPyS** were recorded in the presence/absence of  $\beta$ -CD or  $\gamma$ -CD. Proton NMR spectra of **CoPyS** in  $\text{D}_2\text{O}$  were recorded varying mole fractions of  $[\text{CoPyS}]/([\text{CoPyS}] + [\text{CD}])$  from 0 to 1. As the mole fraction increased, pronounced up-field changes in chemical shift were observed (Fig. S1, ESI<sup>†</sup>). In the presence of  $\beta$ -CD, the meta-proton peak of  $\text{py-SO}_3^-$  in **CoPyS** clearly positive-shifted. In the case of  $\gamma$ -CD, similar peak shifts were observed for the meta-protons and the ortho-protons, where the ortho-protons showed more significant peak shifts compared with the meta-protons. Job plots (Fig. 3) indicated a maximum at a 0.5 mole fraction for either  $\beta$ -CD or  $\gamma$ -CD. Thus, **CoPyS** forms 1:1 inclusion complexes with  $\beta$ -CD or  $\gamma$ -CD. ESI-MS spectra of the mixtures of **CoPyS**/ $\beta$ -CD and **CoPyS**/ $\gamma$ -CD in  $\text{H}_2\text{O-MeOH}$  also supported the formation of 1:1 **CoPyS**-CD inclusion complexes: found  $m/z = 1616.45$  for  $[\text{CoPyS} + \beta\text{-CD}]^-$  (calcd. 1617.75) and  $m/z = 1778.52$  for  $[\text{CoPyS} + \gamma\text{-CD}]^-$  (calcd. 1779.89).

Detailed analysis on proton chemical shifts of 4-py $\text{SO}_3^-$  in **CoPyS** allowed us to determine association constants ( $K_a$ ) of the 1:1 **CoPyS**-CD inclusion complexes. Nonlinear least-square fitting<sup>54</sup> of changes of the proton chemical shifts provided  $K_a$  values of  $81 \pm 23 \text{ M}^{-1}$  for  $\beta$ -CD and  $1600 \pm 400 \text{ M}^{-1}$  for  $\gamma$ -CD (Fig. 4). The  $K_a$  value for  $\gamma$ -CD is 20 times as large as that for  $\beta$ -CD. As mentioned above, the cavity of  $\gamma$ -CD is larger than that of  $\beta$ -CD, and the formation of the inclusion complex of **CoPyS** with  $\gamma$ -CD resulted in the drastic changes in chemical shift of the ortho-H of 4-py $\text{SO}_3^-$ , which is closer to the metal center than the meta-H. Thus, it is most likely that **CoPyS** is placed more deeply inside the  $\gamma$ -CD cavity than inside the  $\beta$ -CD cavity, leading to the higher  $K_a$  value for  $\gamma$ -CD.

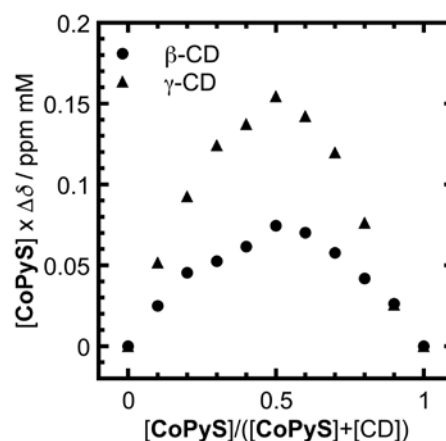


Fig. 3 Job plots for **CoPyS** with  $\beta$ -CD (filled circles) or  $\gamma$ -CD (filled triangles) based on the changes in the proton chemical shifts recorded in  $\text{D}_2\text{O}$ , where  $[\text{CoPyS}] + [\text{CD}] = 4 \text{ mM}$ . The changes of the meta-H of  $\text{py-SO}_3^-$  are plotted for  $\beta$ -CD and those of the ortho-H for  $\gamma$ -CD.

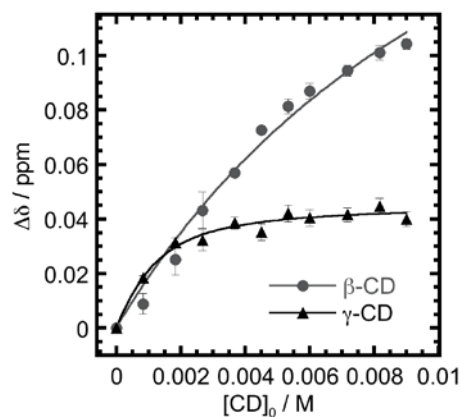


Fig. 4 Changes in chemical shift of the meta-protons of the axial ligand of 4-pySO<sub>3</sub><sup>-</sup> of **CoPyS** upon addition of β-CD or γ-CD in D<sub>2</sub>O. The solid lines indicate the best fit of the data assuming the formation of the 1:1 **CoPyS**-CD complex. The nonlinear least-square curve fitting provided  $K_a = 81 \pm 23 \text{ M}^{-1}$  and  $\Delta\delta_{11} = 0.26 \pm 0.05 \text{ ppm}$  for β-CD and  $K_a = 1600 \pm 400 \text{ M}^{-1}$  and  $\Delta\delta_{11} = 0.046 \pm 0.002 \text{ ppm}$  for γ-CD.

To study the photocatalytic activity of **CoPyS**, visible light-driven hydrogen evolution experiments were performed in aqueous solution at pH 7 containing **CoPyS** (0.18 mM), water-soluble eosin Y (EY, 0.36 mM; Fig. 1) as a photosensitizer and triethanolamine (TEOA, 0.74 M) as a sacrificial electron donor. Time-courses of hydrogen evolution were recorded under visible light irradiation ( $\lambda > 420 \text{ nm}$ ) at 298 K (Fig. 5). The CD-free system produced  $8.5 \pm 0.3 \mu\text{mol}$  of hydrogen after 60 min of the light irradiation, corresponding to  $\text{TON}_{\text{Co}} = 47 \pm 2$ . This photocatalytic activity is comparable with that of a cobaloxime complex with pyridyl-4-phosphonate previously reported.<sup>41</sup> Control experiments revealed that no hydrogen production was observed in the absence of **CoPyS** or EY under the light irradiation, indicating that the co-presence of **CoPyS** and EY is necessary for photochemical hydrogen production because **CoPyS** has almost no UV-Vis absorption band at  $>420 \text{ nm}$  (Fig. S2) and visible-light-driven electron transfer from EY to **CoPyS** initiates hydrogen evolution.

Finally, we investigated effects of host-guest interactions between **CoPyS** and CDs on the photocatalytic hydrogen evolution. Time-courses of hydrogen evolution catalyzed by **CoPyS**-EY systems were recorded in the presence/absence of the α-CD, β-CD or γ-CD (Fig. 5). The presence of γ-CD (0.54 mM) in the reaction solution improved the photocatalytic activity of **CoPyS** ( $9.9 \pm 0.2 \mu\text{mol}$  of hydrogen produced after 60 min of the visible light irradiation, corresponding to  $\text{TON}_{\text{Co}} = 55 \pm 1$ ), compared with the CD-free system. Irradiation of monochromatic light ( $\lambda = 520 \text{ nm}$ ,  $10 \text{ mW cm}^{-2}$ ) for one hour gave external quantum yields of 3.3% in the presence of γ-CD and 2.8% in the absence of γ-CD (Fig. S3, ESI<sup>†</sup>). In contrast, the co-presence of the α-CD (0.54 mM) or β-CD (0.54 mM) with **CoPyS** showed no positive effect on the catalytic activity of **CoPyS**. These results indicate that the host-guest interactions between **CoPyS** and γ-CD gave the positive effect on the hydrogen evolution activity, but not for α-CD or β-CD.

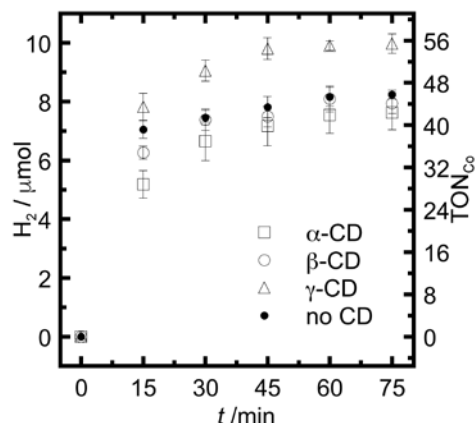


Fig. 5 Time courses of visible light-driven hydrogen evolution catalyzed by **CoPyS** (0.18 mM) and EY (0.36 mM) in the presence of α-CD (0.54 mM, open squares), β-CD (0.54 mM, open circles) or γ-CD (0.54 mM, open triangles) and in the absence of cyclodextrins (filled circles) in buffered aqueous solution (pH 7) containing 0.74 M TEOA under Ar. Visible light ( $\lambda > 420 \text{ nm}$ ) is irradiated.

We observed the positive effect on the catalytic activity of **CoPyS** through the host-guest chemistry with γ-CD. Unfortunately this effect was much less than those reported previously, where an inclusion complexes between β-CD and a diiron model complex of the [FeFe]-hydrogenase active site.<sup>46,47</sup> Although the detailed mechanism on the catalytic activity improvement remain unclear even in the diiron complex system, the hydrophilic hydroxyl rims of the cyclodextrin were able to interact with the guest molecule through hydrogen bonds,<sup>55</sup> leading to the improvement. Thus, the small positive effect on our system is possibly due to the difficulty in interacting the catalytic active site of **CoPyS** and rims of γ-CD. On the basis of the proposed reaction mechanism on cobaloximes [Co<sup>III</sup>(Hdmg)<sub>2</sub>LX] (L = pyridine derivatives, X = halide or labile ligands),<sup>56,57</sup> the hydrogen evolution reaction occurs at the axial position of X, which is on the opposite side of the pyridinyl ligand L. As mentioned above, the axial 4-pySO<sub>3</sub><sup>-</sup> ligand of **CoPyS** is included into γ-CD. In other words, the hydrogen evolution site X is placed away from the rims of the γ-CD. The arrangement of the active site and the rims might result in the small host-guest enhancement in hydrogen evolution activity of **CoPyS**. Another reason on the small positive effect is that the host-guest enhancement can be induced by kinetic effects rather than by thermodynamic effects. Cyclic voltammograms (CVs) of **CoPyS** were recorded in neutral aqueous solution in the presence/absence of γ-CD, indicating almost no difference (Fig. S4). Thus, the host-guest enhancement in hydrogen evolution activity may be governed by kinetic effects. Because EY can be included into γ-CD,<sup>46</sup> the inclusion of not only **CoPyS** but also EY into γ-CD can suppress the electrostatic repulsion between negatively charged **CoPyS** and EY.

## Conclusions

We have investigated host–guest chemistry and visible light-driven hydrogen evolution of the cobaloxime compound with CDs. The cobaloxime formed the 1:1 host–guest complex with  $\beta$ -CD or  $\gamma$ -CD, but not with  $\alpha$ -CD because of the size matching between the CD and **CoPyS**. The association constant of **CoPyS** with  $\gamma$ -CD was approximately 20 times as high as that with  $\beta$ -CD. The inclusion of **CoPyS** into  $\gamma$ -CD enhanced the visible light-driven hydrogen evolution activity, although no enhancement was observed for  $\alpha$ -CD or  $\beta$ -CD. The enhancement comes from kinetic factors including the suppression of the electrostatic repulsion between the negatively charged **CoPyS** and EY.

Our work implies that improving the catalytic activity of cobaloximes through host–guest assembly with CDs requires ligands that provide intermolecular interactions between the catalytic active site and the rim of CDs. For example, equatorial glyoxime ligands can be functionalized with sulfonic acid groups, making the catalytic active site closer to the rim. To develop CD–cobaloxime host–guest systems with high catalytic activity, design and synthesis of new molecular catalysts is underway in our group.

## Experimental

### Materials.

TEOA hydrochloride was purchased from Tokyo Chemical Industry (TCI) Co., Ltd. The other chemicals including Eosin Y sodium salt (EY) were commercially available from Wako Pure Chemical Industries, Ltd. Compounds of 4-pySO<sub>3</sub>H<sup>52</sup> and [Co<sup>III</sup>Cl<sub>2</sub>(Hdmg)(dmg)] (Hdmg = dimethylglyoximate)<sup>51</sup> were prepared according to the literature.

### Synthesis of CoPyS.

Triethylamine (NEt<sub>3</sub>; 21  $\mu$ L, 0.15 mmol) was added into a suspension of [CoCl<sub>2</sub>(Hdmg)(H<sub>2</sub>dmg)] (54 mg, 0.15 mmol) in methanol (4 mL) and the mixture was stirred for 5 min at room temperature to obtain a brown solution. Into this solution, 4-pyridine sulfonic acid (4-pySO<sub>3</sub>H; 24 mg, 0.15 mmol) was added, and then the reaction mixture was stirred at 313 K for 2 h. The reaction mixture was cooled to room temperature and ethyl acetate (ca. 2 mL) was added. After a couple of hours, white precipitates appeared and then were removed by suction filtration. The solvent was removed from the filtrate under vacuum to obtain the product, which was recrystallized from MeOH/AcOEt, followed by MeOH/hexane to obtain brown crystals. The crystals were filtered off and dried under vacuum to obtain 38.9 mg (0.063 mmol, 42%) of **CoPyS** (HNEt<sub>3</sub>[Co<sup>III</sup>Cl(Hdmg)<sub>2</sub>(4-pySO<sub>3</sub>)]). Crystals for single crystal X-ray analysis were grown from a MeOH–hexane mixture solution containing the product. <sup>1</sup>H NMR in D<sub>2</sub>O (400 MHz):  $\delta$  7.66 (2H, 4-pySO<sub>3</sub><sup>-</sup>), 8.20 (2H, 4-pySO<sub>3</sub><sup>-</sup>), 3.21 (6H, NCH<sub>2</sub>CH<sub>3</sub>), 1.30 (9H, NCH<sub>2</sub>CH<sub>3</sub>), 2.44 (12 H, –CH<sub>3</sub>). Elemental analysis for CoC<sub>20</sub>H<sub>38</sub>N<sub>6</sub>SO<sub>8</sub>Cl (**CoPyS**·MeOH) requires C, 38.93%; H, 6.21%, and N, 13.62%. Found: C, 38.24%; H, 5.65%; N, 14.24%. ESI-MS

(MeOH), +ve: found  $m/z$  = 102.13 (requires 102.2 for HNEt<sub>3</sub><sup>+</sup>); –ve: found  $m/z$  = 482.00 (requires 482.77 for [Co<sup>III</sup>Cl(Hdmg)<sub>2</sub>(4-pySO<sub>3</sub>)]<sup>-</sup>).

### Single crystal X-ray analysis.

Single crystal X-ray data of (HNEt<sub>3</sub>)[Co<sup>III</sup>Cl(Hdmg)<sub>2</sub>(4-pySO<sub>3</sub>)]·MeOH were collected on a Bruker SMART Apex II CCD diffractometer with graphite-monochromated Mo K $\alpha$  radiation ( $\lambda$  = 0.71073 Å). The crystal structure was solved by using direct methods (SHELXS-2013) and refined by using full-matrix least-squares methods on  $F^2$  (SHELXL-2014) with the APEX II software. All non-hydrogen atoms were refined anisotropically. The positions of the hydrogen atoms were calculated and refined isotropically.

### Physical measurements.

Proton NMR spectra were recorded on a JEOL JNM-EX400 spectrometer. D<sub>2</sub>O was used as the solvent and all <sup>1</sup>H NMR spectra were calibrated against the residual proton peak of H<sub>2</sub>O.

UV-Vis absorption spectra were obtained using a UV-VIS-NIR spectrophotometer SolidSpec-3700 DUV (SHIMAZU) and Milli-Q water was used as the solvent.

Cyclic voltammograms were recorded on a potentiostat CompactStat (Ivium) using a conventional three-electrode setup. A Ag|AgCl (sat. KCl) as the reference electrode, a pyrolytic graphite edge electrode (BAS) as the working electrode and a platinum foil coated with platinum black as the counter electrode were used. An aqueous solution containing 0.74 M TEOA and 0.1 M NaCl at pH 7 was used as the electrolyte solution. The cyclic voltammograms were recorded at a scanning rate of 0.02 V s<sup>-1</sup> under Ar.

### Job plots of CoPyS with the CDs.

In order to determine host–guest stoichiometry of the inclusion complexes of **CoPyS** with  $\beta$ - or  $\gamma$ -CD, <sup>1</sup>H NMR spectra of **CoPyS** were recorded at 295 K varying mole fractions [CoPyS]/([CoPyS]+[CD]) in D<sub>2</sub>O. The total concentration of ([CoPyS] + [CD]) for each sample was kept to be 4 mM.

### Determination of association constants (K<sub>a</sub>) for the CoPyS–CD inclusion complexes.

Proton NMR spectra of **CoPyS** (0.3 mM) in D<sub>2</sub>O were recorded at 295 K varying concentrations of  $\beta$ -CD or  $\gamma$ -CD. Changes in the proton chemical shifts ( $\Delta\delta_{obs}$ ) of the 4-pySO<sub>3</sub><sup>-</sup> ligand (meta-H) upon addition of CD were plotted against the concentrations of CD ([CD]<sub>0</sub>) and then the data were fitted using the following equation<sup>54</sup>:

$$\Delta\delta_{obs} = \frac{\Delta\delta_{11}}{2K_a[CoPyS]_0} [1 + K_a[CD]_0 + K_a[CoPyS]_0 - \{(1 + K_a[CD]_0 + K_a[CoPyS]_0)^2 - 4K_a^2[CoPyS]_0[CD]_0\}^{\frac{1}{2}}]$$

where  $\Delta\delta_{11}$  is the difference in the chemical shift of the 1:1 **CoPyS**–CD complex with the free **CoPyS** and  $K_a$  is an association constant for the 1:1 **CoPyS**–CD complex.

### Photochemical hydrogen production experiments.

A xenon light source MAX-303 (300W, Asahi Spectra Co., Ltd.) equipped with a mirror module for visible light irradiation (450 nm–800 nm) was used as a light source. To obtain a visible light with  $\lambda > 420$  nm, a long-pass filter LUX422 (Asahi Spectra Co., Ltd.) was used. To obtain green light at  $\lambda = 520$  nm ( $\pm 2$  nm) for quantum yield experiments, a band pass filter MX0520 (Asahi Spectra Co., Ltd.) was used. Light intensities were measured using an analog power meter PM30 (THORLABS, Inc.) with a power sensor S120UV (THORLABS, Inc.).

To quantify the amount of hydrogen produced, a gas chromatograph GC-8A (Shimadzu) with a TCD detector was used. Temperatures were set to be 50°C for an injection port and to be 40°C for a column oven. A molecular sieves 5A column (3 m long) was used. Ar was flowed through the column as a carrier gas.

For photochemical experiments, TEOA buffered solution (0.74 M) at pH 7 was used. A total volume of the solution used for photochemical experiments was 1 mL. The experimental solution was placed in a vial and sealed with a silicone septum, where the sealed vial had a volume of 7.21 mL. The solution was purged with Ar for at least 15 min in the dark before light-driven hydrogen production measurements. The reaction vial was placed in a water jacket filled with water at 298 K during the photochemical experiments. A head-space gas of 100  $\mu$ L was injected into the GC using a gas tight syringe. All photochemical experiments were repeated at least three times in the same condition.

To determine quantum yields for photocatalytic hydrogen evolution, photochemical experiments were performed under light irradiation at 520 nm with 10 mW  $\text{cm}^{-2}$  at 298 K. Quantum yields ( $\phi$ ) were determined based on the following equation<sup>46</sup>:

$$\phi\left(\frac{1}{2}\text{H}_2\right) = 2 \frac{n(\text{H}_2) \times N}{F_{\text{photon}} \times S_{\text{Beam}} \times t} = 2 \frac{n(\text{H}_2) \times N \times h \times c}{P \times \lambda \times t}$$

where  $n(\text{H}_2)$  is the amount of hydrogen produced,  $N$  is the Avogadro constant ( $6.022 \times 10^{23} \text{ mol}^{-1}$ ),  $F_{\text{photon}}$  is a photon flux,  $S_{\text{Beam}}$  is the beam area ( $2.1 \text{ cm}^2$  for our experiments)  $h$  is Planck's constant ( $6.626 \times 10^{-34} \text{ J s}$ ),  $c$  is the speed of light ( $2.9979 \times 10^8 \text{ m s}^{-1}$ ),  $P$  is the light intensity ( $2.1 \text{ cm}^2 \times 0.01 \text{ W cm}^{-2} = 0.021 \text{ W} = 0.021 \text{ J s}^{-1}$ ),  $\lambda$  is the wave length of the light irradiation ( $520 \times 10^{-9} \text{ m}$ ) and  $t$  is the irradiation period ( $60 \text{ min} \times 60 = 3600 \text{ s}$ ).

### Acknowledgements

The authors would like to thank Prof. Katsuaki Konishi, Prof. Yukatsu Shichibu and Dr. Mizuho Sugiuchi (Hokkaido University) for technical supports on single crystal X-ray analysis. We would also like to thank Prof. Yuichi Kamiya, Prof. Nobuo Sakairi, Prof. Tatsuya Morozumi and Mr. Hikaru Nakata (Hokkaido University) for fruitful discussion on experimental setups for the light-driven hydrogen evolution and the determination of the association constants. This work was supported by Grant-in-Aid for Young Scientists (B) (No. 16K20882 to M.K.) and MEXT Program for Development of Environmental Technology using

Nanotechnology from the Ministry of Education, Culture, Sports, Science and Technology, Japan.

### References

1. M. K. Debe, *Nature*, 2012, **486**, 43-51.
2. Z. W. Seh, J. Kibsgaard, C. F. Dickens, I. B. Chorkendorff, J. K. Nørskov and T. F. Jaramillo, *Science*, 2017, **355**, eaad4998.
3. R. W. Hogue, O. Schott, G. S. Hanan and S. Brooker, *Chem. Eur. J.*, 2018, **24**, 9820-9832.
4. W. T. Eckenhoff, *Coord. Chem. Rev.*, 2018, **373**, 295-316.
5. S. Fukuzumi, Y. M. Lee and W. Nam, *Coord. Chem. Rev.*, 2018, **355**, 54-73.
6. J. Willkomm, K. L. Orchard, A. Reynal, E. Pastor, J. R. Durrant and E. Reisner, *Chem. Soc. Rev.*, 2016, **45**, 9-23.
7. K. E. Dalle, J. Warnan, J. J. Leung, B. Reuillard, I. S. Karmel and E. Reisner, *Chem. Rev.*, 2019, **119**, 2752-2875.
8. F. Wittkamp, M. Senger, S. T. Stripp and U. P. Apfel, *Chem. Commun.*, 2018, **54**, 5934-5942.
9. F. Möller, S. Piontek, R. G. Miller and U.-P. Apfel, *Chem. Eur. J.*, 2018, **24**, 1471-1493.
10. W. Lubitz, H. Ogata, O. Rudiger and E. Reijerse, *Chem. Rev.*, 2014, **114**, 4081-4148.
11. T. R. Simmons, G. Berggren, M. Bacchi, M. Fontecave and V. Artero, *Coord. Chem. Rev.*, 2014, **270**, 127-150.
12. D. Schilter, J. M. Camara, M. T. Huynh, S. Hammes-Schiffer and T. B. Rauchfuss, *Chem. Rev.*, 2016, **116**, 8693-8749.
13. M. D. Nothling, Z. Y. Xiao, A. Bhaskaran, M. T. Blyth, C. W. Bennet, M. L. Coote and L. A. Connal, *ACS Catal.*, 2019, **9**, 168-187.
14. E. Kuah, S. Toh, J. Yee, Q. Ma and Z. Q. Gao, *Chem. Eur. J.*, 2016, **22**, 8404-8430.
15. J.-N. Rebilly, B. Colasson, O. Bistri, D. Over and O. Renaud, *Chem. Soc. Rev.*, 2015, **44**, 467-489.
16. R. Gramage-Doria, D. Armspach and D. Matt, *Coord. Chem. Rev.*, 2013, **257**, 776-816.
17. V. Artero, M. Chavarot-Kerlidou and M. Fontecave, *Angew. Chem. Int. Ed.*, 2011, **50**, 7238-7266.
18. J. L. Dempsey, B. S. Brunschwig, J. R. Winkler and H. B. Gray, *Acc. Chem. Res.*, 2009, **42**, 1995-2004.
19. W. T. Eckenhoff, W. R. McNamara, P. W. Du and R. Eisenberg, *Biochim. Biophys. Acta-Bioenerg.*, 2013, **1827**, 958-973.
20. S. W. Cao, X. F. Liu, Y. P. Yuan, Z. Y. Zhang, J. Fang, S. C. J. Loo, J. Barber, T. C. Sum and C. Xue, *Phys. Chem. Chem. Phys.*, 2013, **15**, 18363-18366.
21. X. W. Song, H. M. Wen, C. B. Ma, H. H. Cui, H. Chen and C. N. Chen, *RSC Adv.*, 2014, **4**, 18853-18861.
22. N. Kaeffer, J. Massin, C. Lebrun, O. Renault, M. Chavarot-Kerlidou and V. Artero, *J. Am. Chem. Soc.*, 2016, **138**, 12308-12311.
23. M. Bacchi, E. Veinberg, M. J. Field, J. Niklas, T. Matsui, D. M. Tiede, O. G. Poluektov, M. Ikeda-Saito, M. Fontecave and V. Artero, *ChemPlusChem*, 2016, **81**, 1083-1089.
24. S. Chandrasekaran, N. Kaeffer, L. Cagnon, D. Aldakov, J. Fize, G. Nonglaton, F. Balaras, P. Mailley and V. Artero, *Chem. Sci.*, 2019, **10**, 4469-4475.
25. G. G. Luo, Z. H. Pan, J. Q. Lin and D. Sun, *Dalton Trans.*, 2018, **47**, 15633-15645.

26. A. Panagiotopoulos, K. Ladomenou, D. Y. Sun, V. Artero and A. G. Coutsolelos, *Dalton Trans.*, 2016, **45**, 6732-6738.
27. J. Gu, Y. Yan, J. L. Young, K. X. Steirer, N. R. Neale and J. A. Turner, *Nat. Mater.*, 2016, **15**, 456-460.
28. S. Donck, J. Fize, E. Gravel, E. Doris and V. Artero, *Chem. Commun.*, 2016, **52**, 11783-11786.
29. S. Roy, M. Bacchi, G. Berggren and V. Artero, *ChemSusChem*, 2015, **8**, 3632-3638.
30. J. Willkomm, N. M. Muresan and E. Reisner, *Chem. Sci.*, 2015, **6**, 2727-2736.
31. D. W. Wakerley and E. Reisner, *Phys. Chem. Chem. Phys.*, 2014, **16**, 5739-5746.
32. W. K. Tang, Z. W. Xu, J. Xu, F. Tang, X. X. Li, J. J. Dai, H. J. Xu and Y. S. Feng, *Org. Lett.*, 2019, **21**, 196-200.
33. Z. Liu, Q. C. Du, H. B. Zhai and Y. Li, *Org. Lett.*, 2018, **20**, 7514-7517.
34. R. Zhiani, A. Es-Haghi, S. M. Saadati and S. M. Sadeghzadeh, *J. Organomet. Chem.*, 2018, **877**, 21-31.
35. K. C. Cartwright and J. A. Tunge, *ACS Catal.*, 2018, **8**, 11801-11806.
36. H. Cao, H. M. Jiang, H. Y. Feng, J. M. C. Kwan, X. G. Liu and J. Wu, *J. Am. Chem. Soc.*, 2018, **140**, 16360-16367.
37. X. L. Yang, J. D. Guo, T. Lei, B. Chen, C. H. Tung and L. Z. Wu, *Org. Lett.*, 2018, **20**, 2916-2920.
38. X. Hu, G. T. Zhang, F. X. Bu, X. Luo, K. B. Yi, H. Zhang and A. W. Lei, *Chem. Sci.*, 2018, **9**, 1521-1526.
39. D. W. Wakerley and E. Reisner, *Energy Environ. Sci.*, 2015, **8**, 2283-2295.
40. N. Kaeffer, A. Morozan and V. Artero, *J. Phys. Chem. B*, 2015, **119**, 13707-13713.
41. F. Lakadamyali, M. Kato, N. M. Muresan and E. Reisner, *Angew. Chem. Int. Ed.*, 2012, **51**, 9381-9384.
42. A. A. Ivanov, C. Falaise, P. A. Abramov, M. A. Shestopalov, K. Kirakci, K. Lang, M. A. Moussawi, M. N. Sokolov, N. G. Naumov, S. Floquet, D. Landy, M. Haouas, K. A. Brylev, Y. V. Mironov, Y. Molard, S. Cordier and E. Cadot, *Chem. Eur. J.*, 2018, **24**, 13467-13478.
43. D. Prochowicz, A. Kornowicz and J. Lewinski, *Chem. Rev.*, 2017, **117**, 13461-13501.
44. O. Bistri and O. Reinaud, *Org. Biomol. Chem.*, 2015, **13**, 2849-2865.
45. H. Li, F. Li, B. B. Zhang, X. Zhou, F. S. Yu and L. C. Sun, *J. Am. Chem. Soc.*, 2015, **137**, 4332-4335.
46. X. Q. Li, M. Wang, D. H. Zheng, K. Han, J. F. Dong and L. C. Sun, *Energy Environ. Sci.*, 2012, **5**, 8220-8224.
47. M. L. Cheng, M. Wang, S. Zhang, F. Y. Liu, Y. Yang, B. S. Wan and L. C. Sun, *Faraday Discuss.*, 2017, **198**, 197-209.
48. M. L. Singleton, D. J. Crouthers, R. P. Duttweiler, J. H. Reibenspies and M. Y. Darensbourg, *Inorg. Chem.*, 2011, **50**, 5015-5026.
49. M. L. Singleton, J. H. Reibenspies and M. Y. Darensbourg, *J. Am. Chem. Soc.*, 2010, **132**, 8870-8871.
50. M. V. Rekharsky and Y. Inoue, *Chem. Rev.*, 1998, **98**, 1875-1917.
51. W. C. Trogler, R. C. Stewart, L. A. Epps and L. G. Marzilli, *Inorg. Chem.*, 1974, **13**, 1564-1570.
52. S. Ayesa, C. Lindquist, T. Agback, K. Benkestock, B. Classon, I. Henderson, E. Hewitt, K. Jansson, A. Kallin, D. Sheppard and B. Samuelsson, *Biorg. Med. Chem.*, 2009, **17**, 1307-1324.
53. K. Kano, H. Kitagishi, C. Dagallier, M. Kodera, T. Matsuo, T. Hayashi, Y. Hisaeda and S. Hirota, *Inorg. Chem.*, 2006, **45**, 4448-4460.
54. K. Kano, T. Kitae, Y. Shimofuri, N. Tanaka and Y. Mineta, *Chem. Eur. J.*, 2000, **6**, 2705-2713.
55. M. D. Johnson and J. G. Bernard, *Chem. Commun.*, 1996, **32**, 185-186.
56. A. Bhattacharjee, E. S. Andreiadis, M. Chavarot-Kerlidou, M. Fontecave, M. J. Field and V. Artero, *Chem. Eur. J.*, 2013, **19**, 15166-15174.
57. B. H. Solis, Y. X. Yu and S. Hammes-Schiffer, *Inorg. Chem.*, 2013, **52**, 6994-6999.